

Chapter 7: The Electronic Band Structure of Solids

Bloch & Slater

March 2, 2017

Contents

1	Symmetry of $\psi(\mathbf{r})$	2
2	The nearly free Electron Approximation.	4
2.1	The Origin of Band Gaps	7
3	Tight Binding Approximation	10
4	Photo-Emission Spectroscopy	16
5	Anderson Localization	20

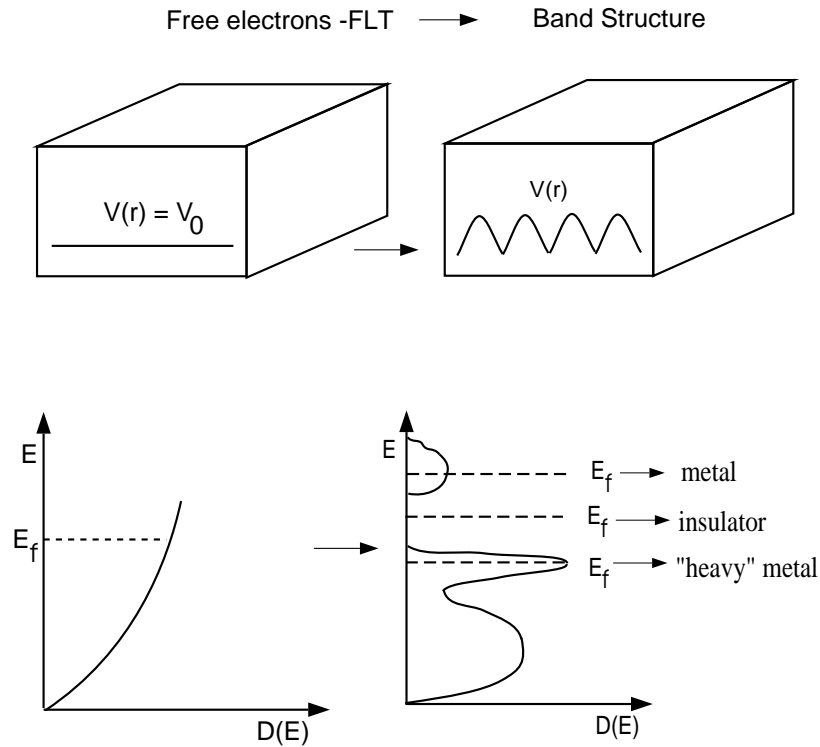


Figure 1: *The additional effects of the lattice potential can have a profound effect on the electronic density of states (RIGHT) compared to the free-electron result (LEFT).*

In the last chapter, we ignored the lattice potential and considered the effects of a small electronic potential U . In this chapter we will set $U = 0$, and consider the effects of the ion potential $V(\mathbf{r})$. As shown in Fig. 1, additional effects of the lattice potential can have a profound effect on the electronic density of states compared to the free-electron result, and depending on the location of the Fermi energy, the resulting system can be a metal, semimetal, an insulator, or a metal with an enhanced electronic mass.

1 Symmetry of $\psi(\mathbf{r})$

From the symmetry of the electronic potential $V(\mathbf{r})$ one may infer some of the properties of the electronic wave functions $\psi(r)$.

Due to the translational symmetry of the lattice $V(r)$ is periodic

$$V(\mathbf{r}) = V(\mathbf{r} + \mathbf{r}_n), \quad \mathbf{r}_n = n_1 \mathbf{a}_1 + n_2 \mathbf{a}_2 + n_3 \mathbf{a}_3 \quad (1)$$

and may then be expanded in a Fourier expansion

$$V(\mathbf{r}) = \sum_{\mathbf{G}} V_{\mathbf{G}} e^{i\mathbf{G}\cdot\mathbf{r}}, \quad \mathbf{G} = h\mathbf{g}_1 + k\mathbf{g}_2 + l\mathbf{g}_3, \quad (2)$$

which, since $\mathbf{G} \cdot \mathbf{r}_n = 2\pi m$ ($m \in \mathcal{Z}$) guarantees $V(\mathbf{r}) = V(\mathbf{r} + \mathbf{r}_n)$. Given this, and letting $\psi(\mathbf{r}) = \sum_{\mathbf{k}} C_{\mathbf{k}} e^{i\mathbf{k}\cdot\mathbf{r}}$ the Schroedinger equation becomes

$$H\psi(\mathbf{r}) = \left[-\frac{\hbar^2}{2m} \nabla^2 + V(\mathbf{r}) \right] \psi = E\psi \quad (3)$$

$$\Rightarrow \sum_{\mathbf{k}} \frac{\hbar^2 k^2}{2m} C_{\mathbf{k}} e^{i\mathbf{k}\cdot\mathbf{r}} + \sum_{\mathbf{k}'\mathbf{G}} C_{\mathbf{k}'} V_{\mathbf{G}} e^{i(\mathbf{k}'+\mathbf{G})\cdot\mathbf{r}} = E \sum_{\mathbf{k}} C_{\mathbf{k}} e^{i\mathbf{k}\cdot\mathbf{r}}, \quad \mathbf{k}' \rightarrow \mathbf{k} - \mathbf{G} \quad (4)$$

or

$$\sum_{\mathbf{k}} e^{i\mathbf{k}\cdot\mathbf{r}} \left\{ \left(\frac{\hbar^2 k^2}{2m} - E \right) C_{\mathbf{k}} + \sum_{\mathbf{G}} V_{\mathbf{G}} C_{\mathbf{k}-\mathbf{G}} \right\} = 0 \forall \mathbf{r} \quad (5)$$

Since this is true for any \mathbf{r} , it must be that

$$\left(\frac{\hbar^2 k^2}{2m} - E \right) C_{\mathbf{k}} + \sum_{\mathbf{G}} V_{\mathbf{G}} C_{\mathbf{k}-\mathbf{G}} = 0, \quad \forall \mathbf{k} \quad (6)$$

Thus the potential acts to couple each $C_{\mathbf{k}}$ only with its reciprocal space translations $C_{\mathbf{k}+\mathbf{G}}$ and the problem decouples into N independent problems for each \mathbf{k} in the first BZ. I.e., each of the N problems has a solution which is a sum over plane waves with wave vectors that differ only by \mathbf{G} . Thus the eigenvalues may be indexed by \mathbf{k} .

$$E_{\mathbf{k}} = E(\mathbf{k}), \quad \text{I.e. } \mathbf{k} \text{ is still a good q.n.}! \quad (7)$$

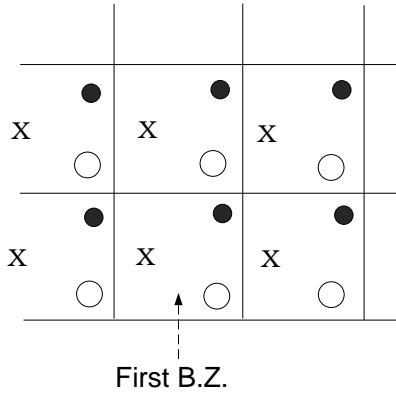


Figure 2: *The potential acts to couple each $C_{\mathbf{k}}$ with its reciprocal space translations $C_{\mathbf{k}+\mathbf{G}}$ (i.e. $x \rightarrow x$, $\bullet \rightarrow \bullet$, and $\circ \rightarrow \circ$) and the problem decouples into N independent problems for each \mathbf{k} in the first BZ.*

We may now sum over \mathbf{G} to get $\psi_{\mathbf{k}}$ with the eigenvector sum restricted to reciprocal lattice sites $\mathbf{k}, \mathbf{k} + \mathbf{G}, \dots$

$$\psi_{\mathbf{k}}(\mathbf{r}) = \sum_{\mathbf{G}} C_{\mathbf{k}-\mathbf{G}} e^{i(\mathbf{k}-\mathbf{G})\cdot\mathbf{r}} = \left(\sum_{\mathbf{G}} C_{\mathbf{k}-\mathbf{G}} e^{-i\mathbf{G}\cdot\mathbf{r}} \right) e^{i\mathbf{k}\cdot\mathbf{r}} \quad (8)$$

$$\psi_{\mathbf{k}}(\mathbf{r}) = U_{\mathbf{k}}(\mathbf{r}) e^{i\mathbf{k}\cdot\mathbf{r}}, \quad \text{where } U_{\mathbf{k}}(\mathbf{r}) = U_{\mathbf{k}}(\mathbf{r} + \mathbf{r}_n) \quad (9)$$

Note that if $V(\mathbf{r}) = 0$, $U(\mathbf{r}) = \frac{1}{\sqrt{V}}$. This result is called *Bloch's Theorem*; i.e., that ψ may be resolved into a plane wave and a periodic function. Its consequences as follows:

$$\begin{aligned} \psi_{\mathbf{k}+\mathbf{G}}(\mathbf{r}) &= \sum_{\mathbf{G}'} C_{\mathbf{k}+\mathbf{G}-\mathbf{G}'} e^{-i(\mathbf{G}'-\mathbf{k}-\mathbf{G})\cdot\mathbf{r}} = \left(\sum_{\mathbf{G}''} C_{\mathbf{k}-\mathbf{G}''} e^{-i\mathbf{G}''\cdot\mathbf{r}} \right) e^{i\mathbf{k}\cdot\mathbf{r}} \\ &= \psi_{\mathbf{k}}(\mathbf{r}), \quad \text{where } \mathbf{G}'' \equiv \mathbf{G}' - \mathbf{G} \end{aligned} \quad (10)$$

I.e., $\psi_{\mathbf{k}+\mathbf{G}}(\mathbf{r}) = \psi_{\mathbf{k}}(\mathbf{r})$ and as a result

$$H\psi_{\mathbf{k}} = E(\mathbf{k})\psi_{\mathbf{k}} \Rightarrow H\psi_{\mathbf{k}+\mathbf{G}} = E(\mathbf{k} + \mathbf{G})\psi_{\mathbf{k}+\mathbf{G}} \quad (11)$$

$$= H\psi_{\mathbf{k}} = E(\mathbf{k} + \mathbf{G})\psi_{\mathbf{k}+\mathbf{G}} \quad (12)$$

Thus $E(\mathbf{k} + \mathbf{G}) = E(\mathbf{k})$: $E(\mathbf{k})$ is periodic then since both $\psi_{\mathbf{k}}(\mathbf{r})$ and $E(\mathbf{k})$ are periodic in reciprocal space, one only needs knowledge of them in the first BZ to know them everywhere.

2 The nearly free Electron Approximation.

If the potential is weak, $V_{\mathbf{G}} \approx 0 \quad \forall \mathbf{G}$, then we may solve the $V_{\mathbf{G}} = 0$ problem, subject to our constraints of periodicity, and treat $V_{\mathbf{G}}$ as a perturbation.

When $V_{\mathbf{G}} = 0$, then

$$E(\mathbf{k}) = \frac{\hbar^2 \mathbf{k}^2}{2m} \quad \text{free electron} \quad (13)$$

However, we must also have that (if $V_{\mathbf{G}} \neq 0$)

$$E(\mathbf{k}) = E(\mathbf{k} + \mathbf{G}) \approx \frac{\hbar^2}{2m} |\mathbf{k} + \mathbf{G}|^2 \quad (14)$$

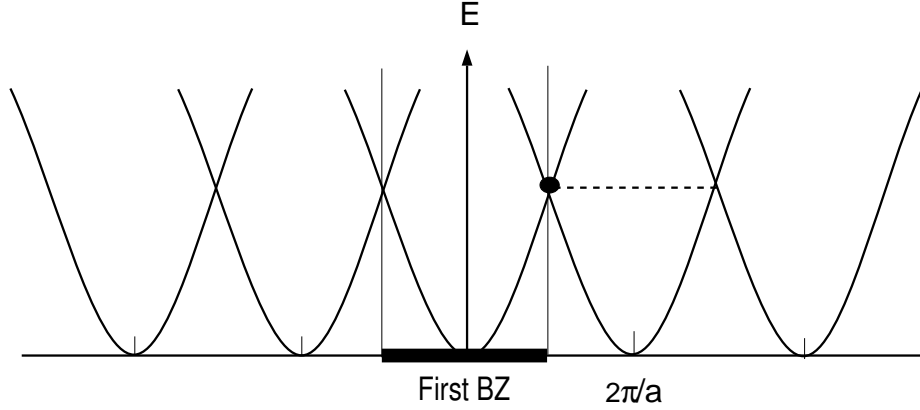


Figure 3: For small $V_{\mathbf{G}}$, we may approximate the band structure as composed of N parabolic bands. Of course, it is sufficient to consider this in the first Brillouin zone, where the parabola centered at finite \mathbf{G} cross at high energies. To understand the effects of the perturbation $V_{\mathbf{G}}$ consider this special \mathbf{k} at the edge of the BZ. where the parabolli cross.

I.e., the possible electron states are not restricted to a single parabola, but can be found equally well on parabolli shifted by any \mathbf{G} vector. In 1-d, since $E(\mathbf{k}) = E(\mathbf{k}+\mathbf{G})$, it is sufficient to represent this in the first zone only. For example in a 3-D cubic lattice the energy band structure along $k_x(k_y = k_z = 0)$ is already rather complicated within the first zone. (See Fig.4.)

The effect of V_G can now be discussed. Let's return to the 1-d problem and consider the edges of the zone where the parabolli intersect. (See Fig. 3.) An electron state with $\mathbf{k} = \frac{\pi}{a}$ will involve *at least* the two \mathbf{G} values $G = 0, \frac{2\pi}{a}$. Of course, the exact solution must involve all \mathbf{G} since

$$\left(\frac{\hbar^2 \mathbf{k}^2}{2m} - E_{\mathbf{k}}\right) C_{\mathbf{k}} + \sum_{\mathbf{G}} V_{\mathbf{G}} C_{\mathbf{k}-\mathbf{G}} = 0 \quad (15)$$

We can generally take $V_0 = 0$ since this just sets a zero for the potential. Then, those

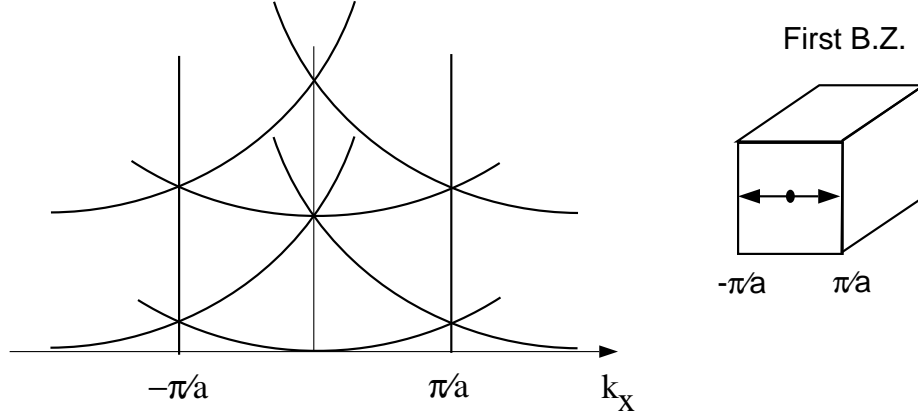


Figure 4: *The situation becomes more complicated in three dimensions since there are many more bands and so they can cross the first zone at lower energies. For example in a 3-D cubic lattice the energy band structure along k_x ($k_y = k_z = 0$) is already rather complicated within the first zone.*

\mathbf{G} for which $E_{\mathbf{k}} = E_{\mathbf{k}-\mathbf{G}} \approx \frac{\hbar^2 \mathbf{k}^2}{2m}$ are going to give the largest contribution since

$$C_{\mathbf{k}} = \sum_{\mathbf{G}} V_{\mathbf{G}} \frac{C_{\mathbf{k}-\mathbf{G}}}{\frac{\hbar^2 \mathbf{k}^2}{2m} - E_{\mathbf{k}-\mathbf{G}}} \quad (16)$$

$$C_{\mathbf{k}} \sim V_{\mathbf{G}_1} \frac{C_{\mathbf{k}-\mathbf{G}_1}}{\frac{\hbar^2 \mathbf{k}^2}{2m} - E_{\mathbf{k}-\mathbf{G}_1}} \quad (17)$$

$$C_{\mathbf{k}-\mathbf{G}_1} = \sum_{\mathbf{G}} V_{\mathbf{G}} \frac{C_{\mathbf{k}-\mathbf{G}_1-\mathbf{G}}}{\frac{\hbar^2 \mathbf{k}^2}{2m} - E_{\mathbf{k}-\mathbf{G}_1-\mathbf{G}}} \quad (18)$$

$$C_{\mathbf{k}-\mathbf{G}_1} \sim V_{-\mathbf{G}_1} \frac{C_{\mathbf{k}}}{\frac{\hbar^2 \mathbf{k}^2}{2m} - E_{\mathbf{k}}} \quad (19)$$

Thus to a first approximation, we may neglect the other $C_{\mathbf{k}-\mathbf{G}}$, and since $V_{\mathbf{G}} = V_{-\mathbf{G}}$ (so that $V(\mathbf{r})$ is real) $|C_{\mathbf{k}}| \approx |C_{\mathbf{k}-\mathbf{G}_1}| \gg \text{other } C_{\mathbf{k}-\mathbf{G}}$

$$\psi_{\mathbf{k}}(\mathbf{r}) = \sum_{\mathbf{G}} C_{\mathbf{k}-\mathbf{G}} e^{i(\mathbf{k}-\mathbf{G}) \cdot \mathbf{r}} \sim \begin{cases} (e^{iGx/2} + e^{-iGx/2}) \sim \cos \frac{\pi x}{a} \\ (e^{iGx/2} - e^{-iGx/2}) \sim \sin \frac{\pi x}{a} \end{cases} \quad (20)$$

The corresponding electron densities are sketched in Fig. 5. Clearly ρ_+ has higher density near the ionic cores, and will be more tightly bound, thus $E_+ < E_-$. Thus a gap opens in E_k near $k = \frac{G}{2}$.

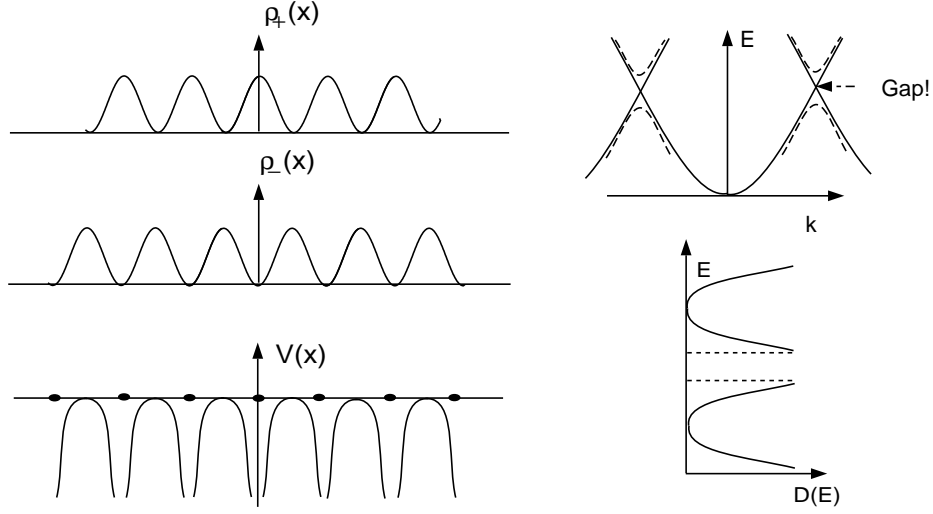


Figure 5: $\rho_+ \sim \cos^2(\pi x/a)$ has higher density near the ionic cores, and will be more tightly bound, thus $E_+ < E_-$. Thus a gap opens in E_k near $k = \frac{G}{2}$.

2.1 The Origin of Band Gaps

Now let's reexamine this gap at $\mathbf{k} = \mathbf{G}_1/2$ in a quantitative manner. Start with the eigen value equation shifted by \mathbf{G} .

$$C_{\mathbf{k}-\mathbf{G}} \left(E_{\mathbf{k}} - \frac{\hbar^2}{2m} |\mathbf{k} - \mathbf{G}|^2 \right) = \sum_{\mathbf{G}'} V_{\mathbf{G}'} C_{\mathbf{k}-\mathbf{G}-\mathbf{G}'} = \sum_{\mathbf{G}'} V_{\mathbf{G}'-\mathbf{G}} C_{\mathbf{k}-\mathbf{G}'} \quad (21)$$

$$C_{\mathbf{k}-\mathbf{G}} = \frac{\sum_{\mathbf{G}'} V_{\mathbf{G}'-\mathbf{G}} C_{\mathbf{k}-\mathbf{G}'}}{\left(E_{\mathbf{k}} - \frac{\hbar^2}{2m} |\mathbf{k} - \mathbf{G}|^2 \right)} \quad (22)$$

To a first approximation ($V_{\mathbf{G}} \simeq 0$) let's set $E = \frac{\hbar^2 \mathbf{k}^2}{2m}$ (a free-electron energy) and ignore all but the largest $C_{\mathbf{k}-\mathbf{G}}$; i.e., those for which the denominator vanishes.

$$\mathbf{k}^2 = |\mathbf{k} - \mathbf{G}|^2, \quad (23)$$

or in 1-d

$$\mathbf{k}^2 = \left(\mathbf{k} - \frac{2\pi}{a} \right)^2 \quad \text{or} \quad \mathbf{k} = -\frac{\pi}{a} \quad (24)$$

This is just the Laue condition, which was shown to be equivalent to the Bragg condition. I.e., the strongest perturbation to the free-electron picture occurs for

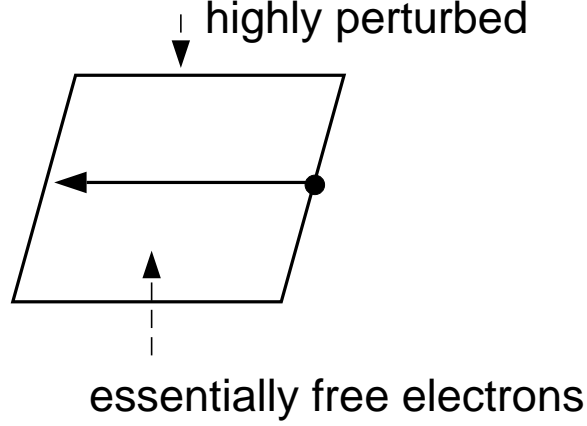


Figure 6: *We can satisfy the condition $E_{\mathbf{k}} \simeq \mathbf{E}_{\mathbf{k}-\mathbf{G}}$ only for \mathbf{k} on the edge of the B.Z.. Here the lattice potential strongly perturbs the electronic states (i.e. more than one $C_{\mathbf{k}-\mathbf{G}}$ is finite).*

states with energies at the edge of the first B.Z. Thus the equation above also tells us that $C_{\mathbf{k}}$ and $C_{\mathbf{k}-\mathbf{G}_1}$ are the most important coefficients (if this electronic state was unperturbed, only $C_{\mathbf{k}}$ would be important). Thus approximately for $V_{\mathbf{G}} \sim 0, V_0 \equiv 0$ and for \mathbf{k} near the zone boundary

$$\mathbf{G} = 0 \quad C_{\mathbf{k}} \left\{ E - \frac{\hbar^2 k^2}{2m} \right\} = V_{\mathbf{G}_1} C_{\mathbf{k}-\mathbf{G}_1} \quad (25)$$

$$\mathbf{G} = \mathbf{G}_1 \quad C_{\mathbf{k}-\mathbf{G}_1} \left\{ E - \frac{\hbar^2 |\mathbf{k} - \mathbf{G}_1|^2}{2m} \right\} = V_{-\mathbf{G}_1} C_{\mathbf{k}}, \quad (26)$$

Again, ignore all other $C_{\mathbf{G}}$. This is a secular equation which has a nontrivial solution iff

$$\begin{vmatrix} \left(\frac{\hbar^2 k^2}{2m} - E \right) & V_{\mathbf{G}_1} \\ V_{-\mathbf{G}_1} & \left(\frac{\hbar^2 |\mathbf{k} - \mathbf{G}_1|^2}{2m} - E \right) \end{vmatrix} = 0 \quad (27)$$

or

$$\begin{vmatrix} E_{\mathbf{k}}^0 - E & V_{\mathbf{G}_1} \\ V_{-\mathbf{G}_1} & E_{\mathbf{k}-\mathbf{G}_1}^0 - E \end{vmatrix} = 0 \quad (28)$$

$$(V_{-\mathbf{G}} = V_{\mathbf{G}}^*, \quad \text{so that } V(\mathbf{r}) \in \mathfrak{R})$$

$$(E_{\mathbf{k}}^0 - E)(E_{\mathbf{k}-\mathbf{G}_1}^0 - E) - |V_{\mathbf{G}_1}|^2 = 0 \quad (29)$$

$$E_{\mathbf{k}}^0 E_{\mathbf{k}-\mathbf{G}_1}^0 - E (E_{\mathbf{k}}^0 + E_{\mathbf{k}-\mathbf{G}_1}^0) + E^2 - |V_{\mathbf{G}_1}|^2 = 0 \quad (30)$$

$$E^{\pm} = \frac{1}{2} (E_{\mathbf{k}-\mathbf{G}_1}^0 + E_{\mathbf{k}}^0) \pm \left\{ \frac{1}{4} (E_{\mathbf{k}-\mathbf{G}_1}^0 - E_{\mathbf{k}}^0)^2 + |V_{\mathbf{G}_1}|^2 \right\}^{\frac{1}{2}} \quad (31)$$

At the zone boundary, where $E_{\mathbf{k}-\mathbf{G}_1}^0 = E_{\mathbf{k}}^0$, the gap is

$$\Delta E = E_+ - E_- = 2|V_{\mathbf{G}_1}| \quad (32)$$

And the band structure looks something like Fig. 7. Within this approximation, the

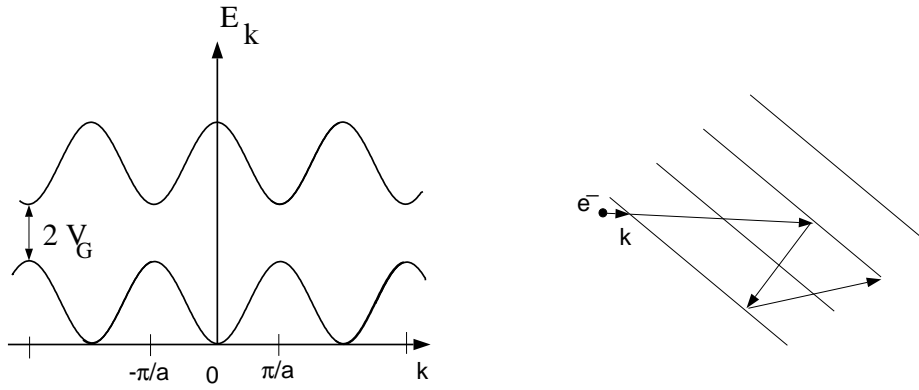


Figure 7:

gap, or forbidden regions in which there are no electronic states arise when the Bragg condition ($\mathbf{k}_f - \mathbf{k}_0 = \mathbf{G}$) is satisfied.

$$|-\mathbf{k}| \approx |\mathbf{k} + \mathbf{G}| \quad (33)$$

The interpretation is clear: the high degree of back scattering for these \mathbf{k} -values destroys the electronic states.

Thus, by treating the lattice potential as a perturbation to the free electron problem, we see that gaps arise due to enhanced electron-lattice back scattering for \mathbf{k} near the zone edge. However, in chapter one, we considered band structure qualitatively and determined that gaps could arise from perturbing about the atomic limit. This in fact, is another natural way of constructing a band structure theory. It is called the tight-binding approximation.

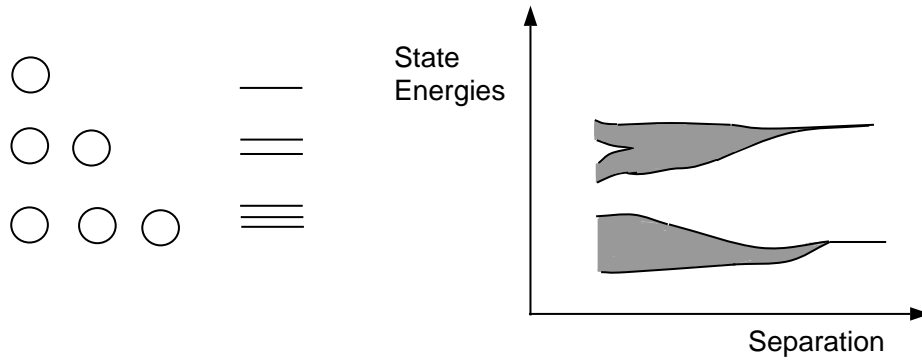


Figure 8: Band gaps in the electronic DOS naturally emerge when perturbing around the atomic limit. As we bring more atoms together (left) or bring the atoms in the lattice closer together (right), bands form from mixing of the orbital states. If the band broadening is small enough, gaps remain between the bands.

3 Tight Binding Approximation

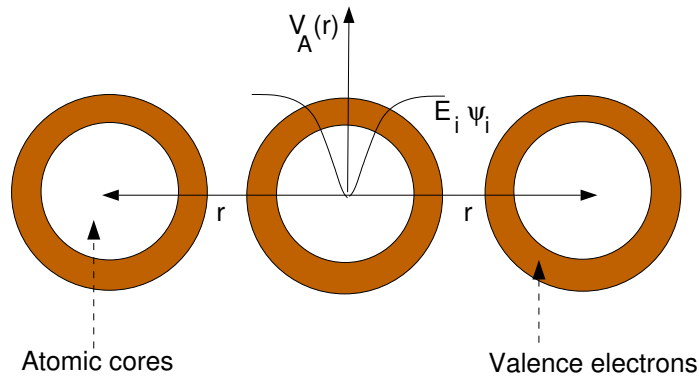


Figure 9: *In the tight-binding approximation, we generally ignore the core electron dynamics and consider only the ionic core potential. For now let's assume that there is only one valence orbital ϕ_i on each atom.*

In the tight-binding approximation, we generally ignore the core electron dynamics and treat consider only the ionic core potential. For now let's assume that there is only one valence orbital ϕ_i on each atom. We will also assume that the atomic problem is solved, and perturb around this solution. The atomic problem has valence

eigenstates ϕ_i , and eigen energies E_i . The unperturbed Schroedinger equation for the n th atom is

$$H_A(\mathbf{r} - \mathbf{r}_n) \cdot \phi_i(\mathbf{r} - \mathbf{r}_n) = E_i \phi_i(\mathbf{r} - \mathbf{r}_n) \quad (34)$$

There is a weak perturbation $v(\mathbf{r} - \mathbf{r}_n)$ coming from the atomic potentials of the other atoms $\mathbf{r}_m \neq \mathbf{r}_n$

$$H = H_A + v = -\frac{\hbar^2 \nabla^2}{2m} + V_A(\mathbf{r} - \mathbf{r}_n) + v(\mathbf{r} - \mathbf{r}_n) \quad (35)$$

$$v(\mathbf{r} - \mathbf{r}_n) = \sum_{\mathbf{m} \neq \mathbf{n}} V_A(\mathbf{r} - \mathbf{r}_m) \quad (36)$$

We now seek solutions of the Schroedinger equation indexed by \mathbf{k} (Bloch's theorem)

$$H\psi_{\mathbf{k}}(\mathbf{r}) = E(\mathbf{k})\Psi_{\mathbf{k}}(\mathbf{r}) \quad (37)$$

$$\Rightarrow \int \psi^* \Rightarrow E(\mathbf{k}) = \frac{\langle \psi_{\mathbf{k}} | H | \psi_{\mathbf{k}} \rangle}{\langle \psi_{\mathbf{k}} | \psi_{\mathbf{k}} \rangle} \quad (38)$$

where

$$\begin{aligned} \langle \psi_{\mathbf{k}} | \psi_{\mathbf{k}} \rangle &\equiv \int d^3\mathbf{r} \psi_{\mathbf{k}}^*(\mathbf{r}) \psi_{\mathbf{k}}(\mathbf{r}) \\ \langle \psi_{\mathbf{k}} | H | \psi_{\mathbf{k}} \rangle &\equiv \int d^3\mathbf{r} \psi_{\mathbf{k}}^*(\mathbf{r}) H \psi_{\mathbf{k}}(\mathbf{r}) \end{aligned} \quad (39)$$

Of course, this problem is almost hopelessly complicated. We cannot solve for $\psi_{\mathbf{k}}$. Rather, we will solve for some $\phi_{\mathbf{k}} \simeq \psi_{\mathbf{k}}$ where the parameters of $\phi_{\mathbf{k}}$ are determined by minimizing

$$\frac{\langle \phi_{\mathbf{k}} | H | \phi_{\mathbf{k}} \rangle}{\langle \phi_{\mathbf{k}} | \phi_{\mathbf{k}} \rangle} \geq E(\mathbf{k}). \quad (40)$$

This is called the Raleigh-Ritz variational principle.

Consistent with our original motivation, we will approximate $\psi_{\mathbf{k}}$ with a sum over atomic states.

$$\psi_{\mathbf{k}} \simeq \phi_{\mathbf{k}} = \sum_{\mathbf{n}} a_n \phi_i(\mathbf{r} - \mathbf{r}_n) = \sum_{\mathbf{n}} e^{i\mathbf{k} \cdot \mathbf{r}_n} \phi_i(\mathbf{r} - \mathbf{r}_n) \quad (41)$$

$$\psi_{\mathbf{k}}(\mathbf{r}) = \mathbf{U}_{\mathbf{k}}(\mathbf{r}) e^{i\mathbf{k} \cdot \mathbf{r}}, \quad \psi_{\mathbf{k}}(\mathbf{r}) = \psi_{\mathbf{k}+\mathbf{G}}(\mathbf{r})$$

Where $\phi_{\mathbf{k}}$ must be a Bloch state $\phi_{\mathbf{k}+\mathbf{G}} = \phi_{\mathbf{k}}$ which dictates our choice $\mathbf{a}_n = e^{i\mathbf{k}\cdot\mathbf{r}_n}$. Thus at this level of approximation we have *no free parameters* to vary to minimize $\langle\phi_{\mathbf{k}}|H|\phi_{\mathbf{k}}\rangle / \langle\phi_{\mathbf{k}}|\phi_{\mathbf{k}}\rangle \approx E(\mathbf{k})$.

Using $\phi_{\mathbf{k}}$ as an approximate state the energy denominator $\langle\phi_{\mathbf{k}}|\phi_{\mathbf{k}}\rangle$, becomes

$$\langle\phi_{\mathbf{k}}|\phi_{\mathbf{k}}\rangle = \sum_{\mathbf{n},\mathbf{m}} e^{i\mathbf{k}\cdot(\mathbf{r}_{\mathbf{n}}-\mathbf{r}_{\mathbf{m}})} \int d^3\mathbf{r} \phi_i^*(\mathbf{r}-\mathbf{r}_{\mathbf{m}}) \phi_i(\mathbf{r}-\mathbf{r}_{\mathbf{n}}) \quad (42)$$

Let's imagine that the valance orbital of interest, ϕ_i , has an very small overlap with adjacent atoms so that

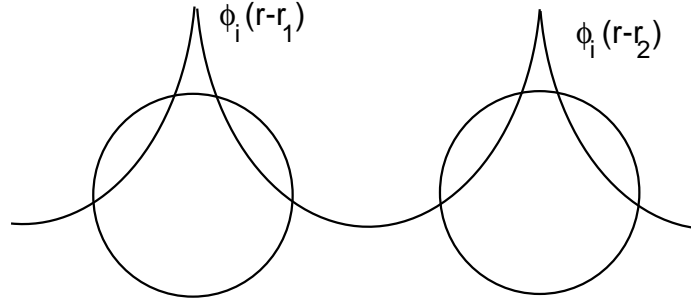


Figure 10: In the tight binding approximation, we assume that the atomic orbitals of adjacent sites have a very small overlap with each other.

$$\langle\phi_{\mathbf{k}}|\phi_{\mathbf{k}}\rangle \simeq \sum_{\mathbf{n}} \int d^3\mathbf{r} \phi_i^*(\mathbf{r}-\mathbf{r}_{\mathbf{n}}) \phi_i(\mathbf{r}-\mathbf{r}_{\mathbf{n}}) = N \quad (43)$$

The last identity follows since ϕ_i is normalized.

The energy for our approximate wave function is then

$$E(\mathbf{k}) \approx \frac{1}{N} \sum_{\mathbf{n},\mathbf{m}} e^{i\mathbf{k}\cdot(\mathbf{r}_{\mathbf{n}}-\mathbf{r}_{\mathbf{m}})} \int d^3\mathbf{r} \phi_i^*(\mathbf{r}-\mathbf{r}_{\mathbf{m}}) \{E_i + v(\mathbf{r}-\mathbf{r}_{\mathbf{n}})\} \phi_i(\mathbf{r}-\mathbf{r}_{\mathbf{n}}). \quad (44)$$

Again, in the first part (involving E_i), we may neglect orbital overlap. For the second term, involving $v(\mathbf{r}-\mathbf{r}_{\mathbf{n}})$, the overlap should be included, but only to the nearest neighbors of each atom (why?). In the simplest case, where the orbitals ϕ_i , are s-orbitals, then we can use this symmetry to reduce the complexity of the problem to

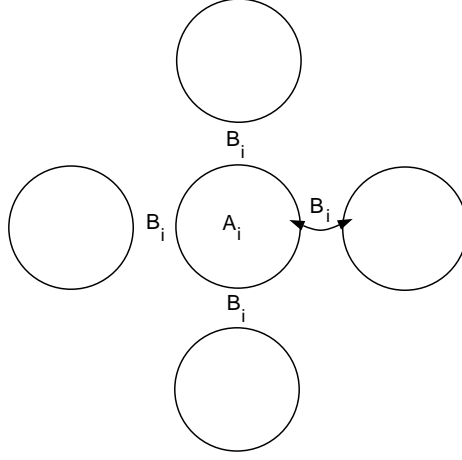


Figure 11: A simple cubic tight binding lattice composed of s-orbitals, with overlap integral B_i .

just two more integrals since the hybridization (B_i) will be the same in all directions.

$$A_i = - \int \phi_i^*(\mathbf{r} - \mathbf{r}_n) v(\mathbf{r} - \mathbf{r}_n) \phi_i(\mathbf{r} - \mathbf{r}_n) d^3 \mathbf{r} \quad \text{ren. } E_i \quad (45)$$

$$B_i = - \int \phi_i^*(\mathbf{r} - \mathbf{r}_m) v(\mathbf{r} - \mathbf{r}_n) \phi_i(\mathbf{r} - \mathbf{r}_n) d^3 \mathbf{r} \quad (46)$$

B_i describes the hybridization of adjacent orbitals.

$$A_i; B_i > 0, \quad \text{since } v(\mathbf{r} - \mathbf{r}_n) < 0 \quad (47)$$

Thus

$$E(\mathbf{k}) \simeq E_i - A_i - B_i \sum_{\mathbf{m}} e^{i\mathbf{k}(\mathbf{r}_n - \mathbf{r}_m)} \quad \text{sum over } \mathbf{m} \text{ n.n. to } \mathbf{n} \quad (48)$$

Now, if we have a cubic lattice, then

$$(\mathbf{r}_n - \mathbf{r}_m) = (\pm a, 0, 0)(0, \pm a, 0)(0, 0, \pm a) \quad (49)$$

so

$$E(\mathbf{k}) = E_i - A_i - 2B_i \{ \cos k_x a + \cos k_y a + \cos k_z a \} \quad (50)$$

Thus a band centered about $E_i - A_i$ of width $12B_i$ is formed. Near the band center, for \mathbf{k} -vectors near the center of the zone we can expand the cosines $\cos ka \simeq 1 -$

$\frac{1}{2}(ka)^2 + \dots$ and let $k^2 = k_x^2 + k_y^2 + k_z^2$, so that

$$E(k) \simeq E_i - A_i + B_i a^2 k^2 \quad (51)$$

The electrons near the zone center act as if they were free with a renormalized mass.

$$\frac{\hbar^2 k^2}{2m^*} = B_i a^2 k^2, \quad \text{i.e. } \frac{1}{m^*} \propto \text{curvature of band} \quad (52)$$

For this reason, the hybridization term B_i is often associated with kinetic energy.

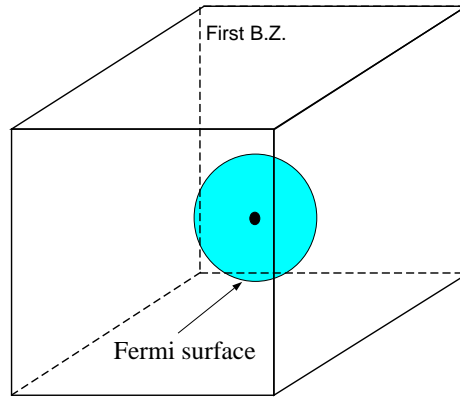


Figure 12: *Electronic states for a cubic lattice near the center of the B.Z. act like free electrons with a renormalized mass. Hence, if the band is partially filled, the Fermi surface will be spherical.*

This makes sense, from its origins of wave function overlap and thus electronic transfer.

The width of the band, $2B_i$, will increase as the electronic overlap increases and the interatomic orbitals (core orbitals or valance f and d orbitals) will tend to form narrow bands with high effective masses (small B_i).

The bands are filled then by placing two electrons in each band state (with spins up and down). A metal then forms when the valence band is partially full. I.e., for Na with a $1s^2 2s^2 2p^6 3s^1$ atomic configuration the 1s, 2s and 2p orbitals evolve into (narrow) filled bands, but the $3s^1$ band will only be half full, and thus it evolves into a metal. Mg $1s^2 2s^2 2p^6 3s^2$ also metal since the p and s band overlaps the unfilled

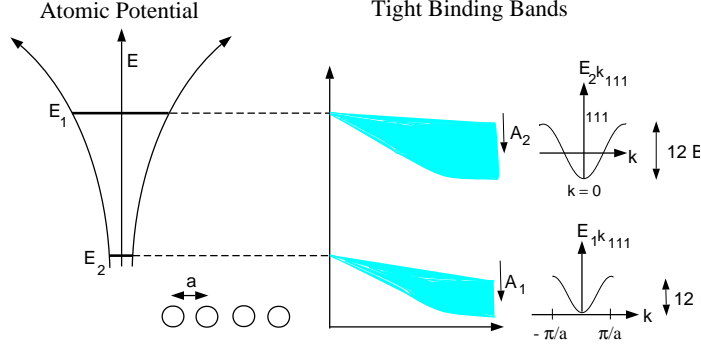


Figure 13: In the tight-binding approximation, bands form from overlapping orbital states (states of the atomic potential). The bandwidth is proportional to the hybridization B ($12B$ for a SC lattice). More localized, compact, atomic states tend to form narrower bands.

d-band. There are exceptions to this rule. Consider C with atomic configuration of $1s^2 2s^2 2p^2$. Its valence s and p states form a strong sp^3 hybrid band which is further split into a bonding and anti-bonding band. (See Fig.14). Here, the gap is not tied to the periodicity of the lattice, and so an amorphous material of C may also display a gap.

The tight-binding picture can also explain the variety of features seen in the DOS of real materials. For example, in Cu (Ar)3d¹⁰4s the d-orbitals are rather small whereas the valence s-orbitals have a large extent. As a result the s-s hybridization B_i^{ss} : is strong and the B_i^{dd} is weak.

$$B_i^{dd} \ll B_i^{ss} \quad (53)$$

In addition the s-d hybridization is inhibited by the opposing symmetry of the s-d orbitals.

$$B_i^{sd} = \int \phi_i^s(\mathbf{r} - \mathbf{r}_1) v(\mathbf{r} - \mathbf{r}_2) \phi_i^d(\mathbf{r} - \mathbf{r}_2) d^3 \mathbf{r} \ll B_i^{ss} \quad (54)$$

where ϕ_i^s is essentially even and ϕ_i^d is essentially odd. So $B_i^{sd} \ll B_i^{ss}$. Thus, to a first approximation the s-orbitals will form a very wide band of mostly s-character and the d-orbitals will form a very narrow band of mostly d-character. Since both

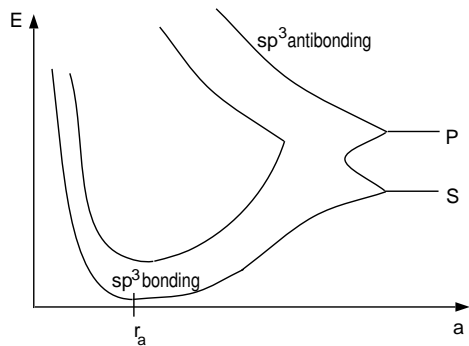


Figure 14: C (diamond) with atomic configuration of $1s^2 2s^2 2p^2$. Its valence s and p states form a strong sp^3 hybrid band which is split into a bonding and anti-bonding band.

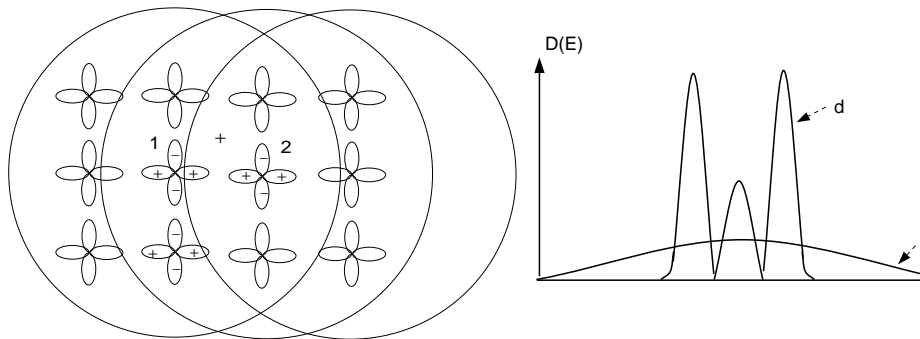


Figure 15: Schematic DOS of Cu $3d^{10}4s^1$. The narrow d-band feature is split due to crystal fields.

the s and d bands are valence, they will overlap leading to a DOS with both d and s features superimposed.

4 Photo-Emission Spectroscopy

The electronic density of electronic states (especially for occupied states), and to a less extent band structure, are very important for illuminating the interesting physics of materials. As we saw in Chap. 6, an enhanced DOS at the Fermi surface indicates an enhanced electronic mass, and if $D(E_F) = 0$, we have an insulator (semiconductor).

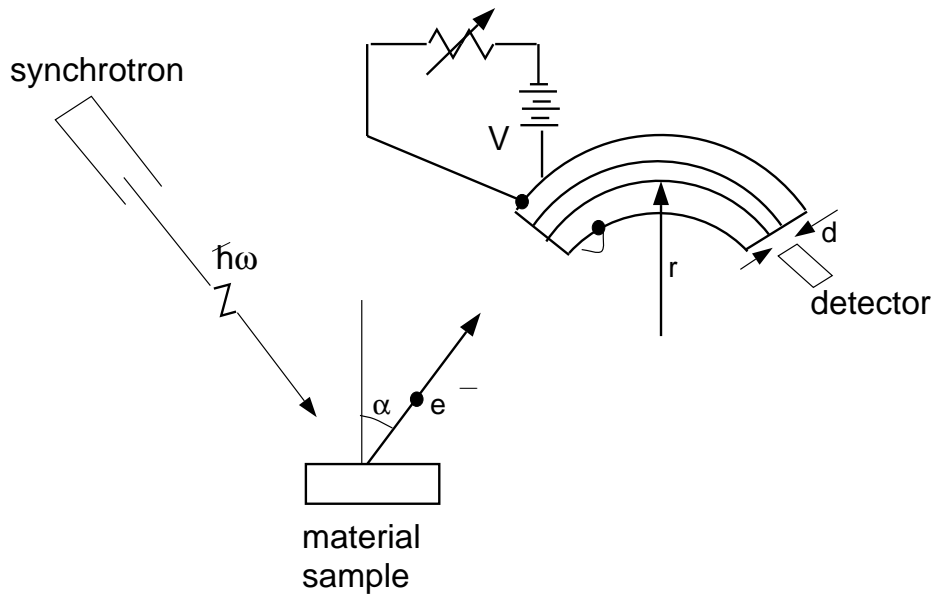


Figure 16: **XPS Experiment:** *By varying the voltage one may select the kinetic energy of the electrons reaching the counting detector.*

The effective electronic mass also varies inversely with the curvature of the bands. The density of states away from the Fermi surface can allow us to predict the properties of the material upon doping, or it can yield information about core-level states. Thus it is important to be able to measure $D(E)$. This may be done by x-ray photoemission (XPS), UPS or PS in general. The band dispersion $E(\mathbf{k})$ may also be measured using angle-resolved photoemission (ARPES) where angle between the incident radiation and the detector is also measured.

The basic idea is that a photon (usually an x-ray) is used to knock an electron out of the system (See figure 17.) Of course, in order for an electron at an energy of E_b below the Fermi surface to escape the material, the incident photon must have an energy which exceeds E_b and the work function ϕ of the material. If $\hbar\omega > \phi$, then the emitted electrons will have a distribution of kinetic energies E_{kin} , extending from zero to $\hbar\omega - \phi$. From Fermi's golden rule, we know that the probability per unit time of an electron being ejected is proportional to the density of occupied electronic

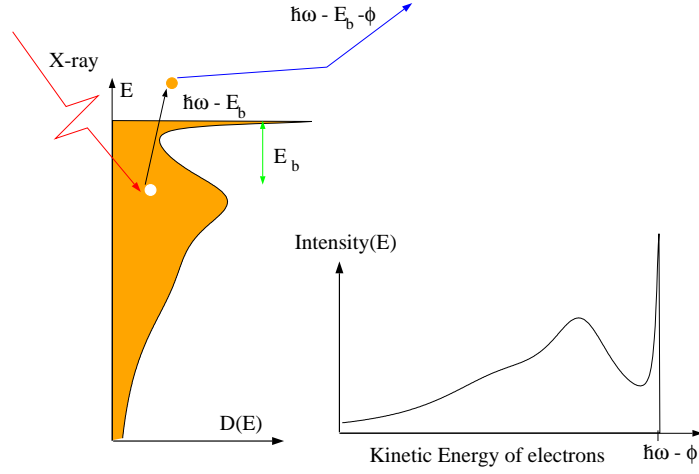


Figure 17: Let the binding energy be defined so that $E_b > 0$, $\phi =$ work function, then the detected electron intensity $I(E_{kin} - \hbar\omega - \phi) \propto D(-E_b)f(-E_b)$

states times the probability (Fermi function) that the electronic state is occupied

$$\begin{aligned}
 I(E_{kin}) &= \frac{1}{\tau(E_{kin})} \propto D(-E_b)f(-E_b) \\
 &\propto D(E_{kin} + \phi - \hbar\omega)f(E_{kin} + \phi - \hbar\omega)
 \end{aligned} \tag{55}$$

Thus if we measure the energy and number of ejected particles, then we know $D(-E_b)$.

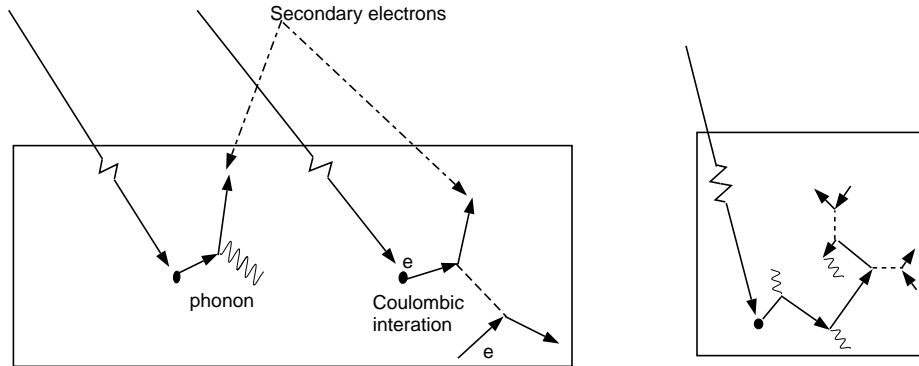


Figure 18: Left: Origin of the background in $I(E_{kin})$. Right: Electrons excited deep within the bulk scatter so often that they rarely escape. Thus, most of the signal I originates at the surface, which must be clean and representative of the bulk.

There are several problems with this procedure. First some of the photon excited

particles will scatter off phonons and electronic excitations within the material. Since these processes can occur over a very wide range of energies, they will produce a broad featureless background in $N(E_{\mathbf{k}})$.

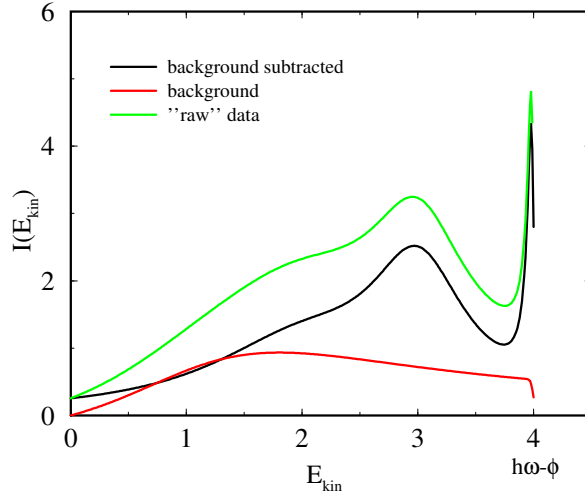


Figure 19: *In Photoemission, we measure the rate of ejected electrons as a function of their kinetic energy. The raw data contains a background. Once this is subtracted off, the subtracted data is proportional to the electronic density of states convolved with a Fermi function $I(E_{kin}) \propto D(E_{kin} + \phi - \hbar\omega)f(E_{kin} + \phi - \hbar\omega)$.*

Second, due to these secondary scattering processes, it is very unlikely that an electron which is excited deep within the bulk, will ever escape from the material. Thus, we only learn about $D(E)$ near the surface of the material. Therefore it is important for this surface to be “clean” so that it is representative of the bulk. For this reason these experiments are often carried out in ultra-high vacuum conditions.

We can also learn about the electronic states $D(E)$ above the Fermi surface, $E > F_F$, using *Inverse Photoemission*. Here, an electron beam is focused on the surface and the outgoing flux of photons are measured. Inverse photoemission has significantly less energy resolution (roughly 100 meV) than PES, which with a laser light source, can be as good as several meV.

5 Anderson Localization

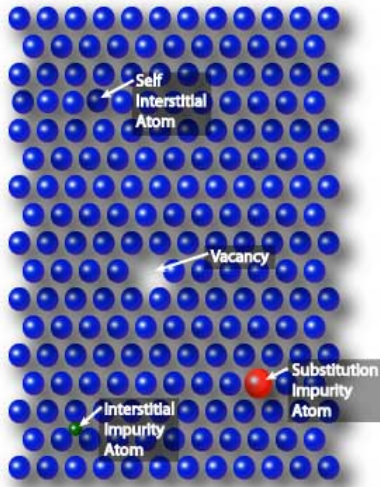


Figure 20: *Examples disorder, including substitution, interstitial, vacancies. In addition, not shown, there are external disorder potentials, amorphous systems, etc.*

In this chapter, we have seen that electrons do not scatter off a perfect periodic lattice, unless the Bragg condition is satisfied opening a band gap. If not, according to Bloch, they form extended states composed of a plane wave multiplied by a periodic function. So, the electronic wavefunction (and charge!) is spread over the entire system with equal amplitude on each site! Such states are characteristic of a metal and are called “extended states”.

On the other hand, we know that the impact of disorder on such a system can be significant. As illustrated in Fig. 20 there are many different types of disorder, including substitutional disorder, as in the replacement of Si by B or P in Si semiconductors used in your laptop which is responsible for roughly one to four trillion dollars of the US economy. Disorder is not a nuisance, rather it is very often used to tune or control the properties of materials.

In fact very strong disorder can even destroy the metal which contains it. This means that Bloch’s theorem, which was derived in the absence of disorder, breaks down and the extended states that are spread over the entire system become exponentially localized states centered at one position in the material. In the most extreme limit, this is obviously true. Consider a single orbital that you pull down in energy so that it falls below (or above) the continuum in the density of states. Clearly, such a state cannot hybridize with other states since there are none at the same energy. Thus, any electron on this orbital is localized, and the electronic DOS at this energy will be a delta function.

Anderson has shown that other types of disorder can lead to the localization of electronic states, as illustrated in Fig. 21. Mott argued that the extended states would be separated from the localized states by a sharp mobility (localization) edge in energy. His argument is

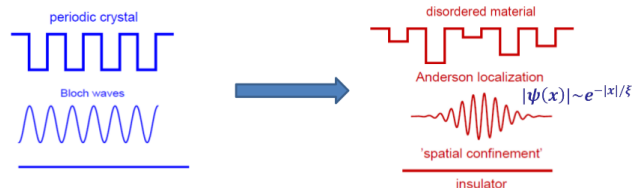


Figure 21: A periodic potential (left) leads to extended states; whereas, strong disorder will lead to exponentially localized states (right).

that scattering from disorder is elastic, so that the incoming wave and the scattered wave have the same energy. On the other hand, nearly all scattering potentials will scatter electrons from one wavevector to all others, since the scattering potentials are local or nearly so. If two states, corresponding to the same energy and different wavenumbers exist, then the scattering potential will cause them to mix, causing both to become extended.

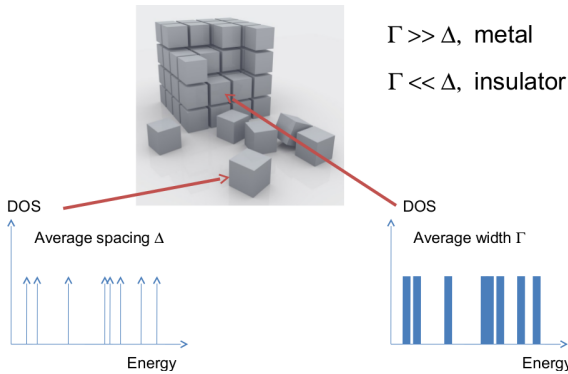


Figure 22: To understand localization, divide a system up into blocks. The average spacing of the energy levels of a block is Δ and the Fermi golden rule width of the levels is Γ . If $\Gamma \gg \Delta$ then we have a metal and if $\Gamma \ll \Delta$, an insulator).

These ideas have existed in one form or another for over fifty years! The main remaining challenge is to develop a complete theory of localization. This has been hampered by the lack of a clearly identified order parameter, akin to m in the theory of magnetism! Recently, there has been significant progress along these ideas, with the local typical density of states identified as the order parameter.

To see this, imagine dividing the system up into blocks, as illustrated in Fig. 22. Here the average level spacing of the states in a block is Δ and their average Fermi golden rule width is Γ . If

$\Gamma \gg \Delta$ then we have a metal since the states at this energy have a significant probability of escaping from this block, and the next one. Alternatively if $\Gamma \ll \Delta$ the escape probability of the electrons is low, so that an insulator forms. So what does this mean in terms of the local electronic density of states that are measured (i.e., via STM) at one site in the system? If I measure the DOS at any site in a metal, it must be a continuum, at least at the energy at question, since all states at that energy must be extended and therefore accessible (c.f. Fig. 23). On the other hand, in a insulator, at any one site, the DOS would “see” only the states that are accessible (within the localization length) and since the number of these states is necessarily finite, the DOS at any one site would be composed of a set of delta functions. Of course, if I go to another site, then the distribution of the delta functions will be different, so if I average over all 10^{23} sites, then I again recover a continuum. I.e., the arithmetically averaged DOS is a continuum in both a metal and an insulator.

On the other hand, the typical value of the local DOS in a metal is very different than the typical value in an insulator. Consider again the local DOS in the metal and insulator illustrated in Fig. 23. In the metal, at any one energy the DOS at each site is a continuum. It will change as one goes from site to site, but the typical value, as the average value, will be finite. now reconsider the local DOS in the insulator. It is composed of a finite number of delta functions. For any energy in between the delta functions, the local DOS is zero. Since the number of delta functions is again finite, the typical value of the local DOS is zero. As a result, the order parameter for the Anderson metal-insulator transition is the typical local DOS, which is zero in the insulator and finite

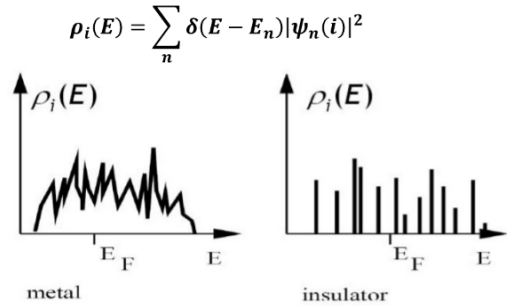


Figure 23: *The local DOS in a metal (left) is a continuum; whereas, that in an insulator is composed of a series of delta functions (right).*

in the metal.

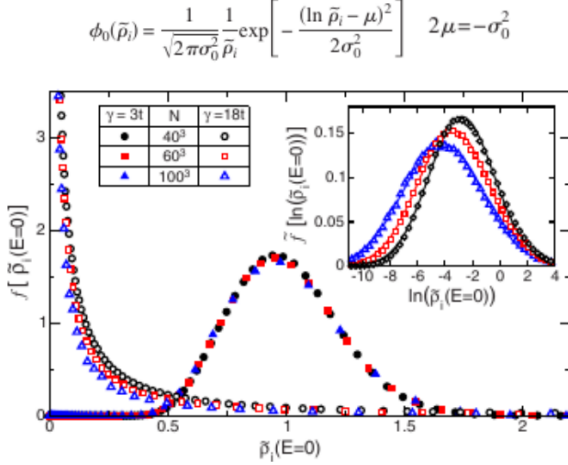


Figure 24: *The distribution of the local density of states in a single-band Anderson model with disorder strength γ . Near the localization transition, $\gamma = 16.5$ the distribution becomes log-normal (see also the inset), while for values well below the transition, $\gamma = 3$ is shown, the distribution is normal.[1].*

A stronger statement is also possible. Early on, Anderson realized that the distribution of the density of states in a strongly disordered metal would be strongly skewed towards smaller values. More recently, this distribution has been demonstrated to be log normal. Perhaps the strongest demonstration of this fact was by the Vollhardt group[1], who illustrated the the DOS near the transition has a log-normal distribution (Fig. 24) over 10 orders of magnitude! Furthermore, one may also show that the typical value of a log-normal distribution is the geometric average (the geometric average of A and B is \sqrt{AB}) which is particularly easy to calculate and can serve as an order parameter.

References

- [1] Gerald Schubert, Jens Schleede, Krzysztof Byczuk, Holger Fehske, and Dieter Vollhardt Phys. Rev. B 81, 155106 Published 8 April 2010.